Supplementary Information for

Femtosecond visible transient absorption spectroscopy of chlorophyll *f*-containing Photosystem II

Noura Zamzam, Rafal Rakowski, Marius Kaucikas, Gabriel Dorlhiac, Sefania Viola, Dennis J. Nürnberg, Andrea Fantuzzi, A. William Rutherford, and Jasper J. van Thor*

Jasper J. van Thor
Email: j.vanthor@imperial.ac.uk

This PDF file includes:

Supplementary text

Figures S1 to S8

SI References

www.pnas.org/cgi/doi/10.1073/pnas.2006016117

Supplementary Information Text

Absorption Spectra of WL-PSII and FR-PSII

Spectra of PSII cores purified from *C. thermalis* PCC 7203 grown under far-red light (FR) were compared with those of PSII cores purified from *T. elongatus* grown under white light (WL). WL-PSII from *T. elongatus* was used instead of WL-PSII from *C. thermalis* PCC 7203 because the latter did not have the purity required for the experiments. The use of PSII cores from a different organism, *T. elongatus*, is justified as all the subunits in the FR-PSII (with the exception of the H-subunit and the extrinsic subunits) are different from those in the WL-PSII and in sequence terms, all the canonical, chlorophyll-*a*-containing, PSII in cyanobacteria are more closely related to each other than to the FR-PSII. The use of *T. elongatus* PSII also allowed comparison with previously reported transient absorption data for PSII core complexes derived from this cyanobacterium. Steady-state absorption spectra of isolated WL-PSII and FR-PSII are presented in Fig. S1. The marked difference between the two spectra is the additional absorption band around 715 nm in the FR-PSII spectrum associated with the far-red light absorbing chlorophyll-*f* pigments and this corresponds to a modified action spectrum for PSII activity (1).

Transient absorption spectra of WL-PSII

Two pump wavelengths were used for WL-PSII: 663 nm pump excites predominantly blue-shifted chl-*a* pigments in the antenna of the PSII core complex, and 675 nm which is preferentially absorbed by antenna chlorophylls at this longer wavelength. The transient absorption data at selected delays for both pump wavelengths are presented in Fig. S2.

At delays close to time zero, the TA spectrum with 663 nm excitation is dominated by a GSB/SE at 676 nm. This characteristic chl-*a* Q_y absorption band is mainly from chl-*a* pigments in the PSII core antenna.

A positive feature at 652 nm, which can be assigned to the excited state absorption of antenna chl-*a* molecules, and broad absorption in the 500-625 nm region are also present. Those features were previously observed in species-associated difference spectra of intact PSII core associated with excited state compartments (2). The 715-800 nm wavelength region does not show any spectral features at this delay.

However, in the 0.3 ps spectrum, a band appears at 780 nm. In addition to this absorption, the maximum of the major GSB/SE shifts to 681 nm and the excited state absorption band at 652 nm decays significantly. The 10 ps spectrum shows a further shift of the GSB/SE band maximum to 684 nm. This red shift and narrowing of the main GSB/SE band, along with excited state absorption at 665 nm, are characteristic of the transfer of excitation energy towards the RC (2).

At 100 ps, the main negative band has further decayed but without change in its peak position at 684 nm. The reduction in the band amplitude might reflect the loss of the contribution from SE due to charge separation. This spectrum also shows that while broadband absorption in the 500-625 nm region decayed significantly, a bleach appeared at 544 nm, which may have started to form in the 10 ps spectrum. This is assigned to the

bleaching of $Pheo_{D1}$ ground state Q_x absorption band, indicating the formation of the $Pheo_{D1}^{-\bullet}$ radical in early kinetic studies (reviewed in (3)) and more recently in ref (2). This assignment means that a charge-separated state is present at this stage. Moreover, the broad absorption at wavelengths longer than 700 nm has been previously associated with the formation of the radical pair states and was observed by Holzwarth et al. in the species-associated difference spectra representing the three radical pair states RP1, RP2, and RP3, which are assigned to $Chl_{D1}^{+\bullet}Pheo^{-\bullet}$, $P680^{+\bullet}Pheo^{-\bullet}$, and $P680^{+\bullet}Q_A^{-\bullet}$ respectively (2).

The 1000 ps spectrum shows a slight blue shift of the main bleach from 684 nm to 683.5 nm which is also indicative of RP3 formation (see Fig. 3D in Ref. (2)).

The biggest difference for transient absorption measurements using 675 nm excitation compared to 663 nm is the lack of significant shifts of the major negative feature at ~680 nm at any of the reported time delays. Its maximum is at 682 nm for the time zero spectrum and shifts to 683 nm for the longer delay spectra. Only the 2000 ps spectrum shows a slight blue shift of the main bleach position to 682 nm.

All other spectral features observed at different time delays are very similar in the two data sets collected with 675 nm and 663 nm excitation. A small, but noticeable exception is the negative feature at 740 nm for 0.5 and 10 ps spectra which is much more pronounced in the 675 nm data. One possible assignment for this feature is stimulated emission (SE) from chl-*a*, a characteristic of excited states of antenna and reaction centre pigments (2). Loss of stimulated emission is expected at longer delay times, marking the decay of excited state associated with the formation of a charge-separated state. However, the shift of more than 50 nm calls the assignment of this band to stimulated emission into question. The other possible assignment for this band is to low energy sites in PSII (4, 5).

Lifetime Density Map of WL-PSII

As the data set collected with 663 nm excitation contains fewer delay points, its lifetime map is less informative, so only the lifetime map for 675 nm excitation data is shown in Fig. S3.

As expected from the spectra, most of the peaks are in the 640-720 nm range. The 500-600 nm part of the spectrum is not shown in the lifetime maps as the signals in this region are weak and are further obstructed by broadband absorption which makes them unsuitable for analysis.

In the first picosecond, there is a spectrally broad signal with positive amplitude followed by a negative feature in the 650-700 nm region with lifetime of 0.4-0.5 ps associated with the initial rise of the GSB/SE around 675 nm followed by its decay. Two small signals can be observed in delays up to 10 ps – positive 2 ps at 665 nm and negative 4 ps at 682 nm. The next prominent negative peak is at the position of the main GSB/SE band in the spectrum and corresponds to a 40-100 ps lifetime. This is the time constant range that is generally observed and reported for experiments involving PSII core complexes and is usually assigned to either antenna-RC transfer (6) or evolution of the charge-separated state (2, 7).

A positive peak at around 500 ps in 640 nm–670 nm range most likely represents the evolution of a charge-separated state. The peak indicates decay in absorption and/or increased bleaching in this region, representing a decay in the excited state and/or the formation of chl-*a* cation in the RC. Finally, the negative peak with lifetime of more than 2000 ps is again at the position of the major bleach. The peak potentially represents a decay in the major bleach as a result of electron transfer from $Pheo_{D1}^{-\bullet}$ to Q_A, hence the formation of RP3.

Comparison of the lifetime map of WL-PSII with 675 nm excitation can be made with previously reported results for the same type of the sample (2). While the lifetime density map is of lower temporal resolution, its major features are very similar to those in Ref. (2) despite different excitation wavelengths (See Fig. 2A in (2)). Namely, a strong 0.1 ps-1 ps negative peak in 670 nm region, a broad negative feature at 40 ps and a negative peak at very long delays are present in the current (Fig. S3) and previously reported (2) maps. There are some differences with regard to smaller features, but interestingly there is a weak positive peak in the 640 nm-670 nm region of both maps –at 150 ps in ref (2), and at 500 ps in the current data.

Homogeneous modelling of WL-PSII TA data

The resulting sequential fit of WL-PSII 675 nm excitation data is presented in Fig. S4. The time constants obtained in this fit are also indicated in the lifetime map in Fig. S3. The model is comparable to earlier work done on similar samples (2). The compartment A spectrum has a time-constant of 1.75 ps and reflects the formation of excited state chl-*a* antenna with the following characteristic features: a major GSB/SE around 682 nm, an excited state absorption around 649 nm, and stimulated emission around 740 nm.

The spectrum of compartment B (Fig. S4) with a 49.6 ps time constant shows only a few new features compared to the previous spectrum. These include a slight reduction in the amplitude of some of the bands arising from excited state absorption and stimulated emission, and a slight narrowing in the major GSB. Compartment B may thus be showing contributions from both decay of excited reaction centre (RC*) state and formation of RP1 ($Chl_{D1}^{+\bullet}Pheo_{D1}^{-\bullet}$). A femtosecond IR study of plant PSII cores (6) assigned a single compartment from their kinetic model to a mixture of RC* and RP1. They were unable to identify a discrete RP1 and this was put down to the low concentration of the radical pair present (6).

Lifetimes similar to that of compartment B (49.6 ps) have been observed in most of the PSII core complex TA studies (2, 6, 8); however, the assignments differ. The transfer-to-trap limited model suggests that this time constant should correspond to excitation transfer from CP43 and CP47 antennae to the RC and thus formation of the RC excited state (6). The trap-limited model, on the other hand, assigns this lifetime to reversible electron transfer between radicals in the RC (2, 7).

Compartment C shows a decay of stimulated emission around 740 nm and a broad absorption beyond 700 nm, both of which are indicative of charge separation. Additionally,

the 540 nm bleach associated with the formation of $Pheo^{-\bullet}$ anion radical is clearly visible in the spectrum, and the minor bleach around 630 nm along with the major bleach at 680 nm are associated with the formation of $P_{D1}^{+\bullet}$. Thus, the third compartment with a lifetime of 495 ps is dominated by spectral features assigned to the formation of $P_{D1}^{+\bullet}Pheo_{D1}^{-\bullet}$, RP2.

In the final spectrum, compartment D, with a lifetime of 6 ns, shows a bandshift around 540 nm and a decay in the major bleach corresponding to electron transfer from $Pheo^{-\bullet}$ to Q_A. The small 630 nm bleach feature is very similar to that observed in the flash-induced $P_{D1}^{+\bullet}Q_A^{-\bullet}$ spectrum at 77 K (9) and the $P_{D1}^{+\bullet}$ spectrum in Mn-depleted PSII preparations (10). Thus, the compartment D spectrum reflects the formation of RP3 ($P_{D1}^{+\bullet}Q_A^{-\bullet}$).

Overall, the spectra and time constants produced by the sequential fit of WL-PSII TA data are similar to those previously reported for this type of sample (2).

Comparison of WL-PSII and 675 nm FR-PSII sequential fits

The initial compartments of the sequential models of WL-PSII (Fig. S4) and the 675 nm FR-PSII model (Fig. 3 in the main text) share the same key features: a major GSB/SE band around 677 nm, excited state absorption at ~650 nm, broad absorption in the 500-650 nm region and at ~780 nm, and stimulated emission at ~740 nm. Both compartments are dominated by features assigned to the formation of excited chl-*a* antenna. One additional compartment in the FR-PSII fit represents excitation energy transfer from antenna chl-*a* to FR pigments. From then on, the spectra of WL-PSII and FR-PSII differ, with the associated time constants being comparable. Distinct bands attributed to FR chlorophylls dominate the FR-PSII spectra. The final nanosecond spectra of both WL-PSII and FR-PSII fits share the bleaches caused by the formation of $P_{D1}^{+\bullet}$, with the pigment being a chl-*a* cation in both systems. However, the bleaches have significantly lower amplitudes in the FR-PSII data. A marked difference between WL-PSII and FR-PSII fits is that the bands in the Pheo Q_x absorption region are barely detectable in the FR-PSII spectra. This observation is rationalised in the discussion section in the main text.

TA spectra of FR-PSII at 27 ns

Figure S5 shows the TA spectra of FR-PSII obtained at 27 ns. At that time delay, the fluorescence contribution should be negligible, and the spectra should essentially reflect a final charge-separated state, RP3. The amplitudes are not comparable with those in the 2 ns and 12 ns spectra (Fig. 2 in the main text) because of the different measuring conditions. However, the spectral features are similar, with the bands appearing at the same positions. Thus, all the spectra in the nanosecond timescale are believed to represent the same state, RP3, with two distinct negative features at 675 nm and 725 nm. The significant reduction in the 725 nm band amplitude in the 12 ns and 27 ns spectra is explained by residual stimulated emission contributions at 2 ns and 12 ns time delays. The attribution of the 675 nm and 725 nm features in the 27 ns spectra to a final charge-separated state, RP3, is further supported by their appearance in the millisecond spectra of FR-PSII presented in Fig. S6.

-100 ps/1 ms spectrum

The spectrum shown in Fig. S6 indicates that the amplitude of the 1 ms spectrum is roughly three times bigger in WL-PSII case. This may also relate to the argument discussed in the main text about the wider distribution of charge separation kinetics in FR-PSII resulting in a lower concentration of the final radical pair state, RP3. This was also manifested in the lower amplitude of the 675 nm bleach associated with $P_{D1}^{+\bullet}$ formation in the 2 ns spectra of FR-PSII (Fig. 2 in main text) compared to WL-PSII (Fig. S2b).

Comparing the relative amplitudes of the 675 nm and 725 nm negative features in the nanosecond spectra (Fig. 2 in main text and Fig. S5) and the millisecond spectra in Fig. S6, it appears that the decay of the 725 nm band with time is more pronounced than that of the 675 nm bleach. Stimulated emission is not thought to be contributing to the 725 nm band at delays as long as 27 ns and longer. Thus, the millisecond spectra indicate that the decay rate of the 725 nm feature, assigned to a $Q_A^{-\bullet}$-induced electrochromic shift on a far-red chlorophyll, is faster than that of the 675 nm bleach caused by the formation of $P_{D1}^{+\bullet}$.

The difference between the FR-PSII millisecond spectra at 675 nm and 720 nm excitations (Fig. S6), with lower amplitudes in the case of the latter, is mostly likely attributable to 720 nm excitation yielding less photochemistry. This would be expected due to the smaller absorption cross section at 720 nm compared to 675 nm as emphasised in the main text.

PSII redox state and annihilation

It has been previously observed that the kinetics of fluorescence and transient absorption are significantly different when PSII is in the closed state, that is when $Q_A^{-\bullet}$ is present before excitation takes place (2, 7, 11, 12). Thus, it is important to consider the conditions of the current experiment in terms of the RC state. Annihilation processes, caused by over-excitation of the sample, can also distort the observed kinetics of the transient absorption signal and thus should also be taken into account (2, 13).

The theoretical model aimed at assessing the effect of annihilation relies on the correct value of the extinction coefficient (13). Using a reasonable estimate for the PSII core complex extinction coefficient in the equations provided by Müller et al. (13) gives an average number of photons per core complex particle in our experiment below 0.5.

Furthermore, the excitation photon flux in the current experiment was below 1.4×10^{14} cm^{-2}. Yoneda et al. showed that at this level of excitation, annihilation does not affect the results significantly (14).

In addition to that, our recently reported TA of PSI results using the same experimental conditions (15) show that for PSI, reducing the pump intensity ten times from current conditions has no effect on the shape of the TA spectra (See Ref. (15) Supplementary Material). Thus, we conclude that the role of annihilation in the current experiment is very small.

As far as the state of the RC is concerned, translation of the sample should provide a fresh sample for each excitation pulse. However, as speed along the Lissajous pattern is not constant, some overlap with previously excited sample cannot be completely avoided.

Hence, we previously assessed the effect of sample translation speed on the resulting spectra using the same excitation conditions as in this experiment (15). The conclusion was that at the speed used in this experiment, the effect of closed centres should be negligible. This is also demonstrated in Figs. S7 and S8. The spectra show a significant reduction in the amplitude of the 675 nm bleach associated with $P_{D1}^{+\bullet}$ formation when measured without sample translation (i.e. in closed centres). In these conditions only 50% of the centres in WL-PSII (and seemingly less in FR-PSII) are expected to perform charge separation resulting in a lower concentration of $P_{D1}^{+\bullet}$.

Moreover, a strong indication of the open state of the RC is the presence of secondary radical pair (RP3) spectral features in the nanosecond WL-PSII spectrum (Fig. S4). Namely, the reduction and slight blue-shift of the main bleach correspond to RP3 formation (2), in addition to the band shift on Pheo Q_x absorption around 540 nm, induced by the formation of $Q_A^{-\bullet}$.

Overall, under the current experimental conditions, the effect of the annihilation and the number of closed RCs in the sample should be rather small.

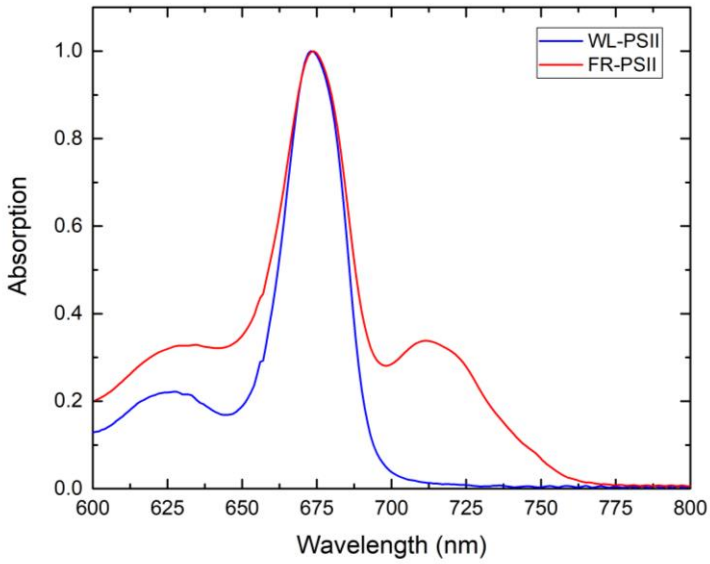

Fig. S1. Steady-state absorption spectra of WL-PSII from *T. elongatus* and FR-PSII from *C. thermalis* PCC 7203. The spectra were normalised to the 675 nm absorption maxima.

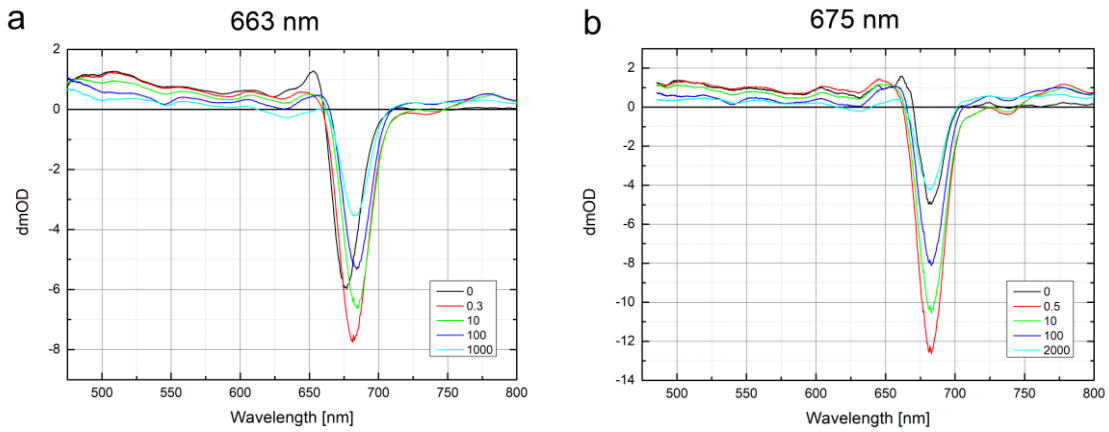

Fig. S2. TA data of WL-PSII at selected delays with two excitation wavelengths: (a) 663 nm and (b) and 675 nm. The delay times in the legend are in picoseconds.

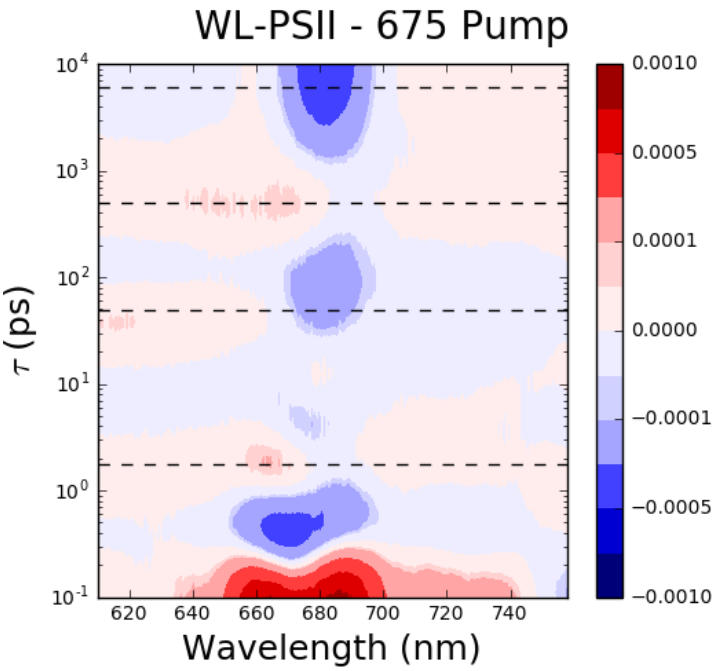

Fig. S3. Lifetime-density map for WL-PSII 675 nm excitation data. Positive amplitudes, represented in red, indicate increased bleaching/stimulated emission or decay of absorption. Negative amplitudes, represented in blue, indicate increased absorption or decay of bleaching/stimulated emission.

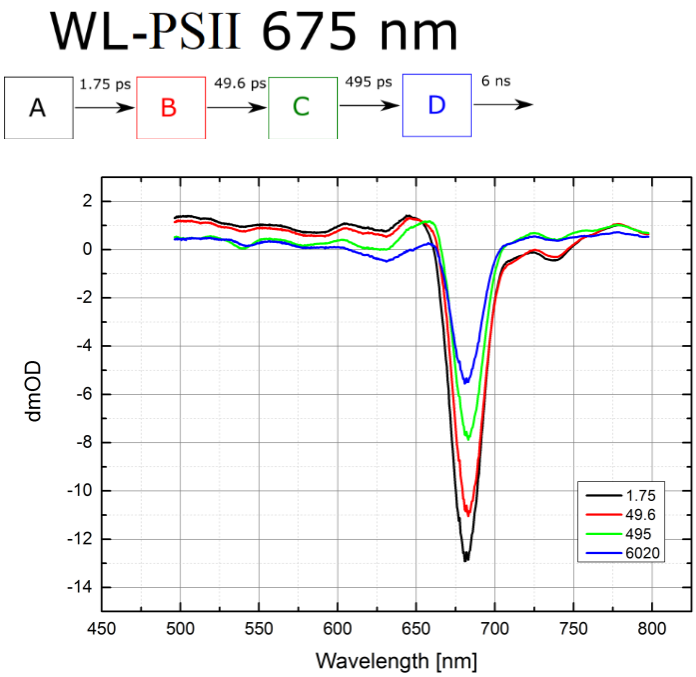

Fig. S4. Results of sequential four compartments fit to WL-PSII 675 nm pump data. The time constants are 1.75 ps, 49.6 ps, 495 ps and 6020 ps.

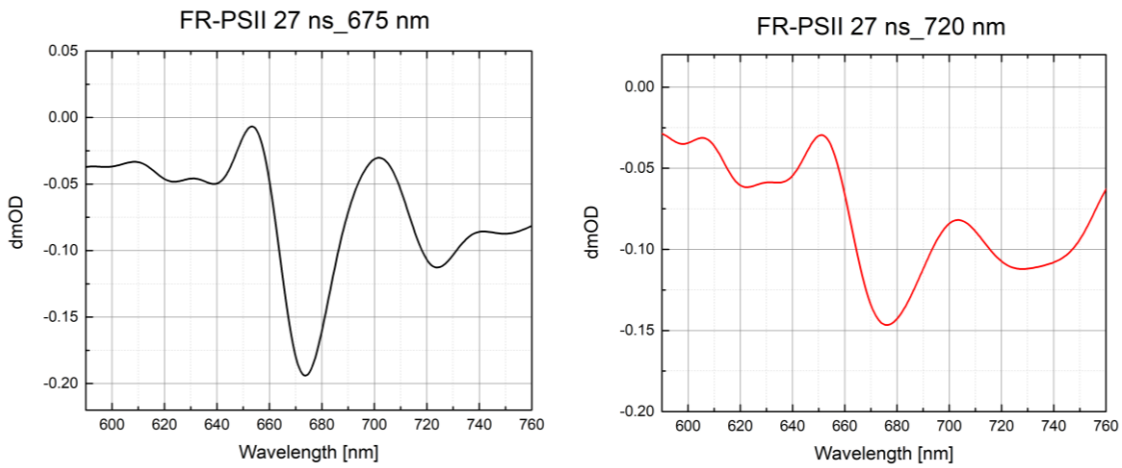

Fig. S5. TA spectra of FR-PSII at 27 ns time delay with 675 nm excitation (left) and 720 nm excitation (right).

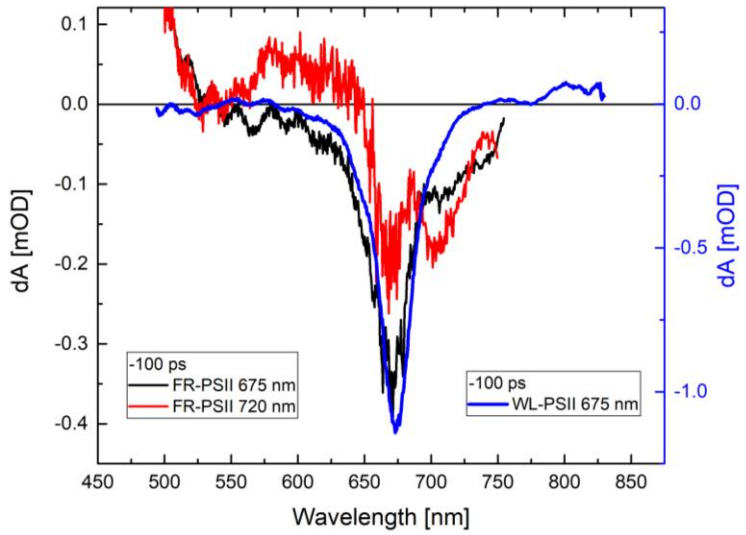

Fig. S6. Millisecond spectra of WL-PSII 675 nm data (blue, right scale), FR-PSII 675 nm (black, left scale) and FR-PSII 720 nm (red, left scale) data.

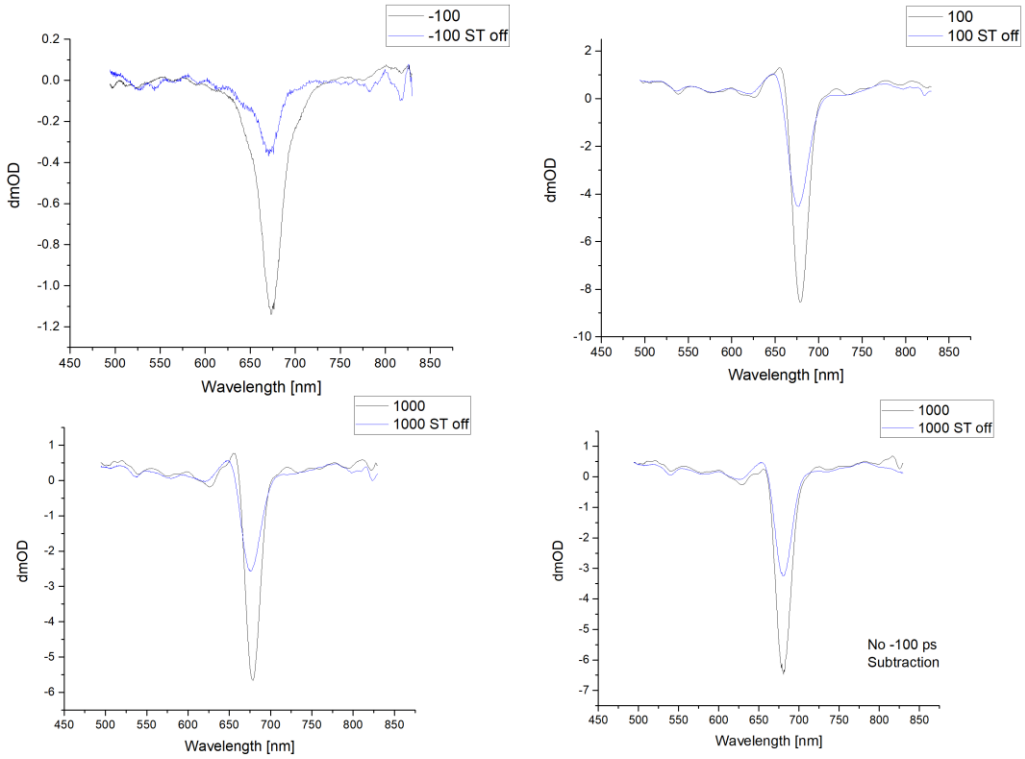

Fig. S7. Effect of sample translation on WL-PSII 675 nm data at different time delays. The bottom right spectrum shows data without subtraction of the -100 ps spectrum. The black spectra were collected with sample translation (ST on) while the blue spectra were collected without sample translation (ST off). The legends show the corresponding time delays in picoseconds.

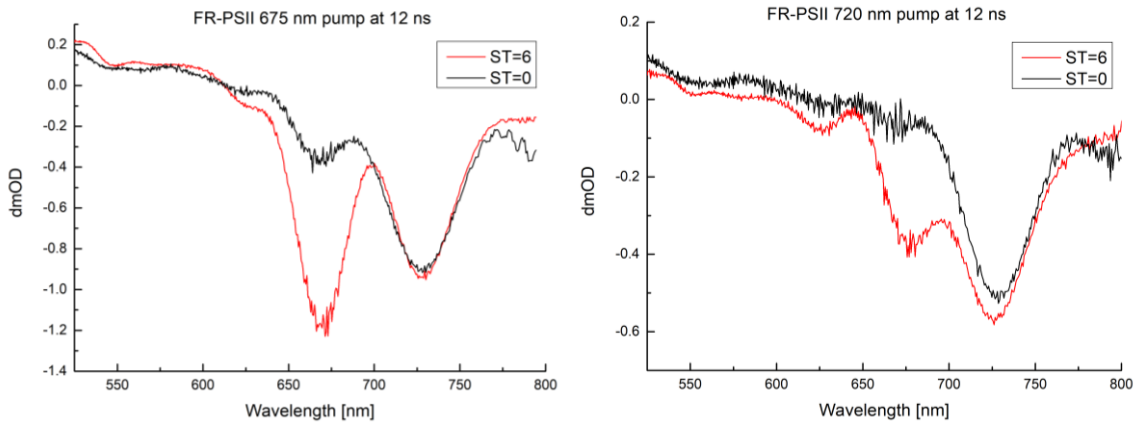

Fig. S8. Effect of sample translation on 12 ns FR-PSII 675 nm and 720 nm data. ST in the legend refers to sample translation speed; ST=0 is the minimum translation speed where the sample is stationary, and ST=6 is the translation speed typically used for the measurements reported in this work.

SI References

1. Nürnberg DJ, et al. (2018) Photochemistry beyond the red limit in chlorophyll f–containing photosystems. *Science* 360(6394):1210–1213.
2. Holzwarth AR, et al. (2006) Kinetics and mechanism of electron transfer in intact photosystem II and in the isolated reaction center: Pheophytin is the primary electron acceptor. *Proc Natl Acad Sci* 103(18):6895–6900.
3. Greenfield SR, Wasielewski MR (1996) Excitation energy transfer and charge separation in the isolated Photosystem II reaction center. *Photosynth Res* 48(1–2):83–97.
4. Reimers JR, et al. (2016) Challenges facing an understanding of the nature of low-energy excited states in photosynthesis. *Biochim Biophys Acta - Bioenerg* 1857(9):1627–1640.
5. Hughes JL, Smith P, Pace R, Krausz E (2006) Charge separation in photosystem II core complexes induced by 690-730 nm excitation at 1.7 K. *Biochim Biophys Acta - Bioenerg* 1757(7):841–851.
6. Pawlowicz NP, Groot M-L, van Stokkum IHM, Breton J, van Grondelle R (2007) Charge separation and energy transfer in the photosystem II core complex studied by femtosecond midinfrared spectroscopy. *Biophys J* 93(8):2732–42.
7. Miloslavina Y, et al. (2006) Charge separation kinetics in intact photosystem II core particles is trap-limited. A picosecond fluorescence study. *Biochemistry* 45(7):2436–2442.
8. Di Donato M, et al. (2008) Primary charge separation in the photosystem II core from Synechocystis: A comparison of femtosecond visible/midinfrared pump-probe spectra of wild-type and two P680 mutants. *Biophys J* 94(12):4783–4795.
9. Hillmann B, Schlodder E (1995) Electron transfer reactions in Photosystem II core complexes from Synechococcus at low temperature - difference spectrum of P680 + Q A- P680 Q A at 77 K. *BBA - Bioenerg* 1231(1):76–88.
10. Allakhverdiev SI, Ahmed A, Tajmir-Riahi HA, Klimov V V, Carpentier R (1994) Light-induced Fourier transform infrared spectrum of the cation radical P680+. *FEBS Lett* 339(1–2):151–154.
11. Schatz GH, Brock H, Holzwarth AR (1988) Kinetic and Energetic Model for the Primary Processes in Photosystem II. *Biophys J* 54(3):397–405.
12. Raszewski G, Renger T (2008) Light Harvesting in Photosystem II Core Complexes Is Limited by the Transfer to the Trap: Can the Core Complex Turn into a Photoprotective Mode? *J Am Chem Soc* 130(13):4431–4446.
13. Müller MG, Hucke M, Reus M, Holzwarth AR (1996) Annihilation processes in the isolated Dl-D2-cyt-b559 reaction center complex of photosystem II. An Intensity-dependence study of femtosecond transient absorption. *J Phys Chem* 100(22):9537–9544.
14. Yoneda Y, Katayama T, Nagasawa Y, Miyasaka H, Umena Y (2016) Dynamics of Excitation Energy Transfer between the Subunits of Photosystem II Dimer. *J Am Chem Soc* 138(36):11599–11605.
15. Kaucikas M, Nürnberg D, Dorlhiac G, Rutherford AW, van Thor JJ (2017) Femtosecond Visible Transient Absorption Spectroscopy of Chlorophyll f - Containing Photosystem I. *Biophys J* 112:234–249.